Colloid Polym Sci (2009) 287:157–165
DOI 10.1007/s00396-008-1959-y

ORIGINAL CONTRIBUTION

Optical properties of molecular aggregates of oxazine dyes in dispersions of clay minerals

Juraj Bujdák · Nobuo Iyi

Received: 23 November 2007 / Revised: 18 June 2008 / Accepted: 26 October 2008 / Published online: 12 November 2008

Abstract The molecular aggregation of oxazine 1 (Ox1) and oxazine 4 (Ox4) in reduced charge montmorillonite (RCM) colloids was investigated by absorption and fluorescence spectroscopies. The aggregation was significantly influenced by the structure of dye cations. Presence of four hydrophobic ethyl groups attached to the ammonium substituents in Ox1 cation prevented formation of closely packed sandwich-type assemblies (*H*-aggregates). Significant effect of the layer charge was observed for Ox4/RCMs dispersions. Large amounts of the Ox4 *H*-aggregates were formed in the systems with RCMs of the highest layer charge and reflected in quenched fluorescence. The presence of *J*-aggregates was proven by absorption spectra for the systems with Ox4 and low-charge RCMs. The flocculation of the lowest charge RCM colloids led to an extensive reduction of the luminescence. The trends and effects of the dye molecular structure and RCM properties are compared with the results previously published for other types of dyes.

Keywords Molecular aggregation · Organic dyes · UV–Vis absorption spectroscopy · Fluorescence spectroscopy · Reduced-charge montmorillonites

N. Iyi
National Institute for Materials Science,
1-1 Namiki,
Tsukuba, Ibaraki 305-0044, Japan

Present address:
J. Bujdák (✉)
Institute of Inorganic Chemistry, Slovak Academy of Sciences,
Dúbravská cesta 9,
845 36 Bratislava, Slovakia
e-mail: uachjuro@savba.sk

Introduction

There are numerous studies dealing with the interaction of clay minerals with organic substances. Significant properties of clay minerals is the adsorption of organic compounds in the form of arranged supramolecular assemblies, clusters, and self-organized molecular aggregates with specific chemical and anisotropic properties [1–3]. Some of organic dyes significantly change their color upon the adsorption at solid/liquid interphases. The phenomenon, historically named metachromasy [4], has been frequently observed in the systems containing organic dyes of flat molecules or chromophoric groups (e.g., methylene blue, thionine) in aqueous colloids containing cells [5] or various polyelectrolytes [6] including biopolymers, such as nucleic acids [7], proteins [8], or polysaccharides [9]. Interestingly, the spectral changes of metachromic dyes are frequently significant. For example, large shifts of absorbed light energies and fluorescence quenching are usually observed [10]. The interpretations of the spectral changes are assigned to the formation of supramolecular assemblies of chromophores with specific structures called molecular aggregates. Individual molecules forming the molecular assemblies are unchanged in this case, which is in contrast to other phenomena, where optical properties of organic dyes are changed upon the reactions (e.g., reactions of pH or redox dye indicators).

Dye molecular aggregation in clay mineral colloids was reported for the first time by Bergman and O'Konski [11]. Since then, numerous papers have been published, studying molecular aggregation of cationic dyes of various types and structures, such as thiazine, rhodamine, cyanine, and triphenylmethane dyes [12]. The changes of dye optical properties in clay mineral dispersions depend much on clay specimen used. Even minerals of the same type and

structure may induce significantly different aggregation of dye molecules [13, 14]. Metachromic dyes had been called "finger-print probes" of surface properties of clays. However, for decades, the effect of clay mineral had not been clearly identified. Later, negative charge of clay mineral layers was identified as a chief parameter, which controls molecular aggregation of cationic dyes [13, 15]. The charge effect was clearly proven in the study of the interaction of reduced charge montmorillonites (RCMs) with methylene blue [13]. The RCMs are semisynthetic clay minerals prepared from one parent material, Li^+-montmorillonite. They are different in layer charge and related properties, but the same in composition and structure [16].

Although the effects of clay mineral properties on dyes molecular aggregation have been described in detail for various types of cationic dyes [12], there is no clear and detail interpretation concerning the influence of dye molecular structure. A few of the parameters already identified or indicated in the older studies include the size and flatness of the dye cation and presence of bulky and/or hydrophobic groups [17].

The objective of this work is a detail investigation of the molecular aggregation of two representative oxazines dyes. Concerning structure and shape of the molecules, oxazines are structurally similar to phenothiazines. The main difference is the presence of oxygen atom and the absence of sulfur atom in a heteroaromatic skeleton of oxazine cations (Fig. 1). This work should answer the questions related to the effect of the structure of oxazines dye cations on the formation of dye molecular assemblies. Oxazines are used as laser dyes [18] and molecular aggregation can be a chief problem for their potential applications in hybrid solid state lasers. On the other hand, controlled formation of luminescent molecular assemblies, such as *J*-type aggregates of a head-to-tail intermolecular association, could lead to the enhancement of emission efficiencies of these fluorophores [10]. The main goal of this work was to clearly identify characteristics of the formation of molecular assemblies of two oxazine dyes in clay mineral aqueous colloids.

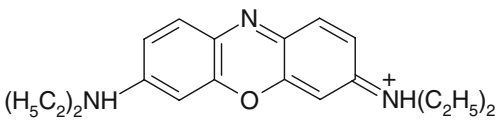

Oxazine 1

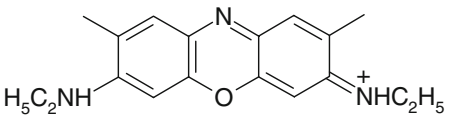

Oxazine 4

Fig. 1 Scheme showing the structure of oxazine dye cations

Experimental

The RCMs were prepared from Li^+-montmorillonite Nanocor (N1), which had been prepared from a commercially available Na^+-saturated form. The Li^+-saturated montmorillonite was prepared by an ion-exchange reaction with LiCl solution. Heat treatment of N was performed at 100 °C, 110 °C, 120 °C, and 130 °C for 24 h to prepare N2–N5 samples with decreasing layer charge. The treatment was carried out in fused silica vessels in a heating box using air atmosphere. The layer charge was characterized by cation exchange capacities (CECs). The CECs were determined as the average number of exchangeable cations per 1 g of dehydrated sample and decreased for the series: 1.35 (N1), 1.24 (N2), 1.18 (N3), 1.14 (N4), and 1.05 mmol/g (N5).

The absorption spectra of the dye/clay dispersions in a UV–Vis region were measured with a V-550 UV–Vis spectrophotometer (Jasco Co., Ltd.). The concentration and loading of the dye cations in the dispersion were always 2.5×10^{-6} mol dm^{-3} and 0.05 mmol g^{-1} clay, respectively. The spectra were measured 1 min and 24 h after mixing the dye solution with the clay dispersion. After 24 h, chemical equilibrium was achieved and the spectra did not change with further aging. The spectra of the clay dispersions without the dye were subtracted from the dye/clay spectra to obtain the spectra for the adsorbed dye species. The positions of the bands were always determined by second derivative spectroscopy. The calculations were combined with Savitzky–Golay smoothing method that performed a local second-order polynomial regression for ten measured points.

The difference spectra (DS) were calculated by subtracting the absorbance values measured for different reaction systems (which were under comparison) for all the wavelengths. The emission spectra were measured on a Shimadzu RF-5000 spectrofluorometer. Only the aged reaction systems were measured after chemical equilibrium had been achieved.

Results and discussion

Figures 2 and 3 show absorption spectra of oxazine dyes in the dispersions of reduced charge montmorillonites. The spectra were measured 1 min (a) and 24 h (b) after mixing the dye solution with clay dispersions. Oxazine 1 (Ox1) spectra do not seem to be significantly affected by the layer

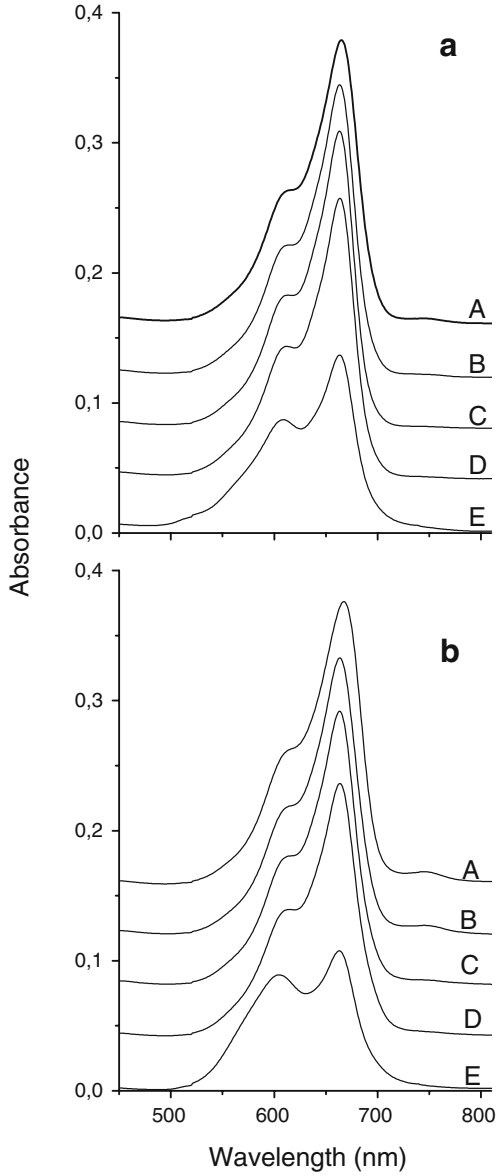

Fig. 2 Absorption spectra of oxazine 1/reduced charge montmorillonite dispersions. The spectra were recorded 1 min (**a**) and 24 h (**b**) after mixing the dye solution with clay mineral dispersions. Reduced charge montmorillonites: N5 (**a**), N4 (**b**), N3 (**c**), N2 (**d**), and N1 (**e**)

charge of clay mineral templates (Fig. 2), especially those measured for freshly prepared dispersions (Fig. 2a). On the other hand, new bands apparently appear in spectra of some oxazine 4 (Ox4)/RCM dispersions (Fig. 3) at both the low and high energies. The presence of these bands is significantly affected by the properties of RCMs. The Ox4 bands at the lowest and highest wavelengths likely represent molecular assemblies of *H*- and *J*-aggregates, respectively. Their positions have been determined using a second derivative spectroscopy, which are analyzed in detail below. The spectra of Ox1 were analyzed in the same way. Although the different trends in Ox1 and Ox4 spectra are apparent, more detail analysis is required in order to characterize molecular aggregation of these dyes in clay mineral dispersions.

Ox4 absorption spectra

All together, five peaks were identified by means of second derivative spectroscopy for Ox4/RCMs colloidal dispersions, whose maximums are located at 486, 575, 604, 628, and 703 nm. Figure 4 shows the second derivative spectra for equilibrated dispersions obtained 24 h after their preparation. The band at 486 nm is assigned to large-size molecular assemblies of an *H*-type with a sandwich-type

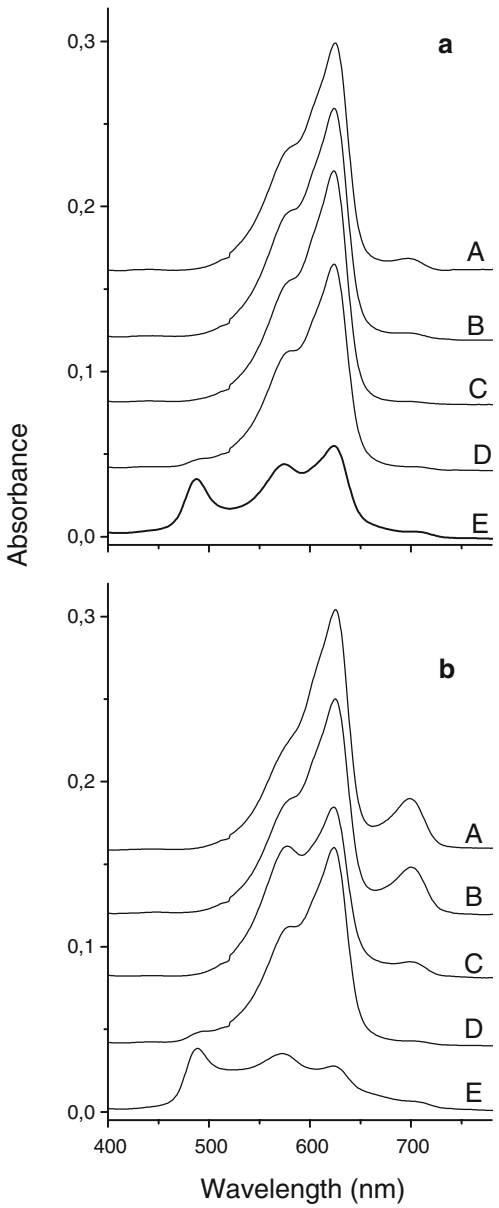

Fig. 3 Absorption spectra of oxazine 4/reduced charge montmorillonite dispersions. The spectra were recorded 1 min (**a**) and 24 h (**b**) after mixing the dye solution with clay mineral dispersions. Reduced charge montmorillonites: N5 (**a**), N4 (**b**), N3 (**c**), N2 (**d**), and N1 (**e**)

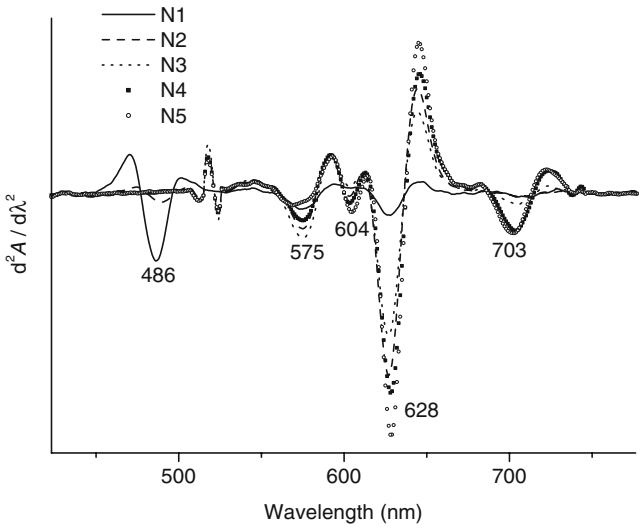

Fig. 4 Second derivative absorption spectra of oxazine 4/reduced charge montmorillonite dispersions. The spectra were recorded 24 h after mixing the dye solution with clay dispersions

structure. This band is clearly detectable for a Ox4/N1 dispersion (Fig. 4, solid line) and visible also in absorption spectrum (Fig. 3, line E). Traces of the *H*-aggregates were detected also for the dispersion with N2 (Fig. 4, dashed line). Any other reaction systems did not exhibit absorption at these wavelengths to be detected by either absorption spectra (Fig. 3) or their second derivatives (Fig. 4). Whereby the *H*-aggregates are formed only in the systems with clay minerals of the highest charge densities (N1, N2), another type of the molecular assemblies called *J*-aggregates and exhibiting maximal light absorption at 703 nm was detected mainly in the systems with the lowest charge RCMs, N3–N5 (Fig. 4, scatters). The *J*-aggregates are the assemblies based on a head-to-tail intermolecular association and their amount increased with the reaction time (Fig. 3).

A dominant band in second derivative spectra (Fig. 4) with the maximum at 628 nm is assigned to isolated dye cations (monomers), common in dilute solutions of this dye. Its position does not significantly change with the layer charge of clay mineral templates. The intensity of this band is variable due to a chemical equilibrium between monomers and molecular assemblies formed via molecular aggregation. The equilibrium of molecular association reaction apparently depends on the layer charge of clay mineral samples. The lowest amount of the monomers is observed for an Ox4/N1 dispersion (Fig. 4, solid line).

In a relatively narrow range of wavelengths, two bands at 575 and 604 nm were clearly detectable using second derivative spectroscopy (Fig. 4). However, there is only one shoulder resolved in absorption spectra being assigned to the band at 575 nm (Fig. 3). Probably, the band at 604 nm overlaps with the main band at 628 nm. One would assume that the band at 604 nm could be associated with the second component of monomers due to a forbidden vibronic transition. The band at 604 nm changes with the layer charge reduction in a similar fashion as the main band, having been assigned to monomers and centered at 628 nm (Fig. 4). The second band at medium wavelengths region near 575 nm can be due to absorption of *H*-dimers. Its evolution with the layer charge does not correlate with the amounts of monomers.

In order to understand the effects of present colloidal particles of RCMs on Ox4 optical properties, DS were calculated (Fig. 5) for equilibrated reaction systems measured after 24 h (Fig. 3). All the spectra show the difference in light absorption between two compared systems with two different RCMs of most similar layer charge. For example, the spectrum of Ox4/N5 was compared with that of Ox4/N4. The difference was calculated by subtraction of the spectrum of the latter system from that of the former one. Positive absorption bands represent forms, which prevail in reaction system with clay mineral of lower charge; the negative ones are assigned to dye species present in higher amounts in the system of a higher charge RCM. The DS for N1 and N2 couple with the peaks of largest intensities indicates the most significant difference. N1 induces formation of relatively more *H*-aggregates compared to N2 (Fig. 5, solid line) which is reflected as a negative band centered at 487 nm. Its position is in accordance to that found using a second derivative spectroscopy shown in Fig. 4. A strong positive band at about 625 nm with a shoulder near 580 nm indicates prevailing formation of monomers and *H*-dimers in the dispersion of lower charge N2. Much stronger

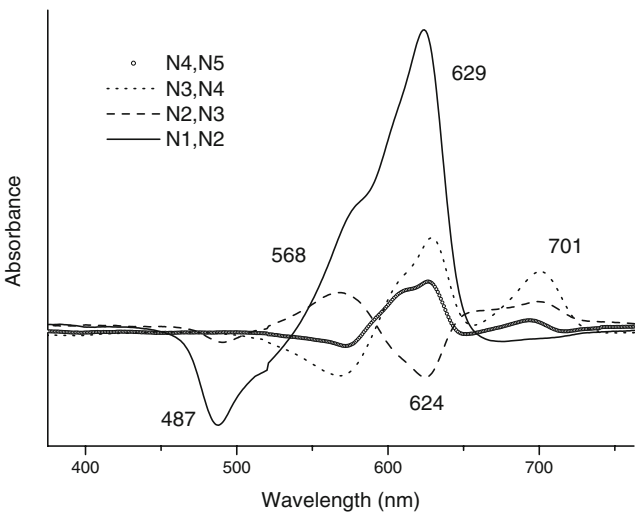

Fig. 5 Difference absorption spectra identifying oxazine 4 species in compared reaction systems. The spectra were recorded 24 h after mixing the dye solution with clay dispersions. Positive and negative bands are assigned to dye species prevailing in the dispersions of reduced charge montmorillonites with lower and higher layer charge, respectively

absorbance of positive absorption indicates larger absorptivity of dye monomers vs. *H*-aggregates, which has been observed for other reaction systems in general [10]. N3, compared to N2, brings about not only to a slight reduction of *H*-aggregates (490 nm) formation but also a partial decrease of the amount of monomers (625 nm; Fig. 5, dashed line). Instead, more *H*-dimers (570 nm) and *J*-aggregates (700 nm) are formed. *H*-dimer band at 568 nm is at lower wavelengths than that identified in second derivative spectra (Fig. 4). Considering the position and broad character of the band at 568 nm indicates the presence of smaller-size *H*-aggregates, including *H*-dimers, prevailing in the Ox4/N3 dispersion. Further charge decrease (N4) led to the reduction of the amount of *H*-dimers and small-size *H*-type assemblies (negative band at 568 nm) in favor of monomers (positive absorption at 624 nm) and *J*-aggregates (700 nm; Fig. 5, dotted line). Similar trend but less extensive changes were observed with further charge reduction as determined from the comparison of Ox4 spectra for N4 and N5 dispersions (Fig. 5, scatter).

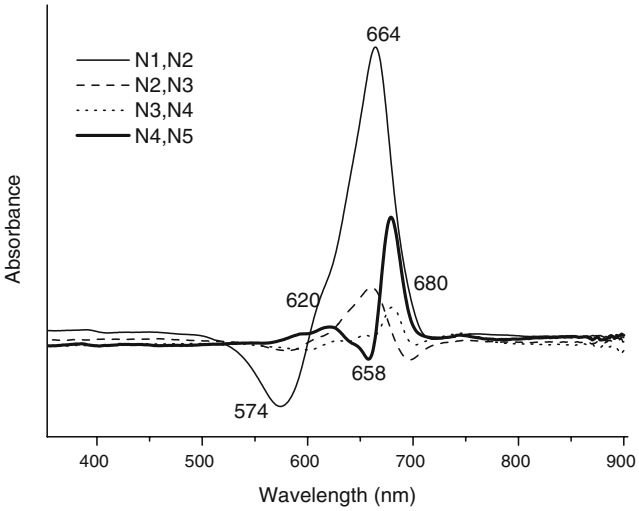

Fig. 7 Difference absorption spectra identifying oxazine 1 species in compared reaction systems. The spectra were recorded 24 h after mixing the dye solution with clay dispersions. Positive and negative bands are assigned to dye species prevailing in the dispersions of reduced charge montmorillonites with lower and higher layer charge, respectively

Ox1 absorption spectra

As mentioned above, only small differences are observed in the Ox1 absorption spectra of RCM dispersions (Fig. 2). The system with N1 exhibits the bands of partially broader shapes and lower intensities. Second derivative spectrum was calculated for equilibrated Ox1/RCMs (Fig. 6) and revealed the existence of three bands, although only two are detectable in absorption spectra (Fig. 2). The three bands occur for all the systems as revealed by second derivative spectroscopy (Fig. 6); the presence of the fourth band at about 700 nm is only indicative. A dominant band assigned to monomers is centered at 666 nm and slightly shifts to lower energies for Ox4/N5 dispersion. The shoulder at 606 nm is assigned to *H*-dimers. The amounts of *H*-dimers are similar for all systems with exception of N1 dispersion (Fig. 6, solid line). The second derivative spectroscopy found out also existence of the band at 638 nm, which is attributed to a forbidden 1-0 vibronic component of the transition of Ox1 monomers. The intensity of this band changes with the charge reduction in a similar trend as observed for the main band of monomers at 666 nm. Clear evidence of larger-size *H*-aggregates has been confirmed by neither absorption spectroscopy (Fig. 2) nor respective second derivative spectra (Fig. 6). This is in contrast to Ox4 dye, which formed *H*-and *J*-aggregates in the systems of clay minerals of high and low layer charge (Figs. 3 and 4). These forms, if they were presents in Ox1/RCMs systems, could be too low in the amount to be detected using absorption spectroscopy, or having been structurally disordered to absorb in a broad range of energies to be identified by the second derivative spectroscopy.

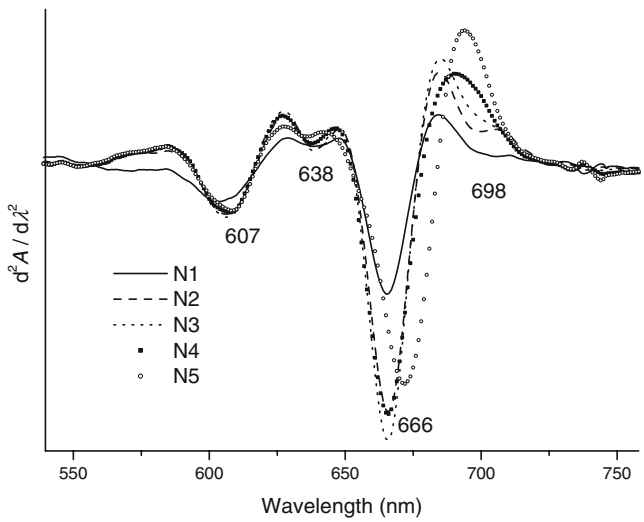

Fig. 6 Second derivative absorption spectra of oxazine 1/reduced charge montmorillonite dispersions. The spectra were recorded 24 h after mixing the dye solution with clay dispersions

DS were calculated in order to identify the differences between the absorption spectra of different reaction systems and to understand the effects of the layer charge reduction on the changes of dye spectral properties (Fig. 7). They were calculated for equilibrated systems in the same way as has been described for Ox4 reaction systems (see discussion above). DS were found to be very useful especially in the case of the systems with Ox1 to identify some of the components. DS for a Ox1/N1 and Ox1/N2 couple was also

calculated for the fresh dispersions (not shown) and revealed the existence of the species absorbing light in a broad range of high energies (at 480–600 nm) prevailing on the surface of higher charge N1. The whole envelope of negative absorption peaks was composed of two relatively broad subunits with the maximums at 525 and 565 nm, respectively. The bands are identified to the *H*-aggregates of variable order and sizes. None of these bands could be detected from Ox1/N1 absorption spectrum (Fig. 2) or its second derivatives (Fig. 6). Absence of any of these peaks in the second derivative can be explained in terms of low intensity and the absorption in a broad range of energies. For aged N1 and N2 dispersions with Ox1, only a single negative nonsymmetric band at low wavelengths was detected (574 nm) indicating prevailing *H*-aggregates in the N1 dispersion (Fig. 7, solid line). Relatively more monomers (positive band at 664 nm) were detected on N2 surface. Formation of the *J*-aggregates (680 nm) was preferred in the systems with low charge RCMs (N4, N5). The positive band at 682 and a shoulder at 748 nm could be associated with *J*-dimers and larger-size *J*-aggregates, respectively. Spectral shift of the main band assigned to the monomers to higher wavelengths (680 nm) cannot be neglected as well. Nevertheless, the largest spectral differences were observed for N1 and N2 systems. The other systems (N2–N5) exhibit relatively similar spectra as indicated by the DS (Fig. 7).

Fluorescence spectroscopy

Fluorescence spectra of Ox4 and Ox1 in the colloidal dispersions of reduced charge montmorillonites are shown in Figs. 8 and 9, respectively. The spectral shape is not significantly related to the properties of clay mineral templates. On the other hand, there are considerable variations of emission efficiencies in dependence on the excitation wavelength, and more importantly, as well as on the layer charge of RCMs.

Ox4 exhibits a nonsymmetric emission with the maximum of about 635 nm (Fig. 8). This value is partially higher than that observed for the dye solution (615 nm) and dye/saponite dispersion (622 nm) as has been observed recently [19]. For the films of montmorillonite with hexadecylammonium cations and this dye, another component at about 665 nm, was identified and assigned to *J*-type molecular assemblies [20]. The band is not clearly resolved in the spectra presented here (Fig. 8), but its presence contributes to the tailing of the main band to higher wavelengths. Interestingly, the spectra can be divided into two groups concerning the intensities of emitted light. First group involves dispersions with medium-charge RCMs (N2–N4). These systems emit light of relatively high intensities. The second group includes the dispersions with

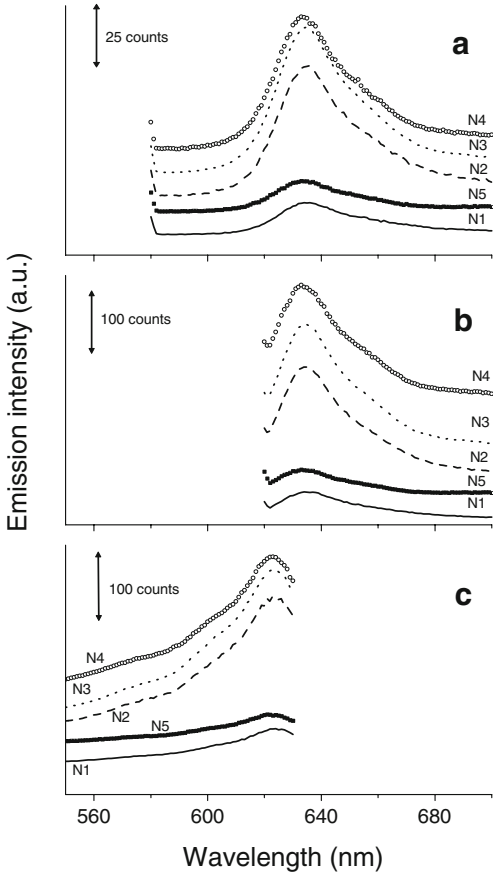

Fig. 8 Fluorescence spectra of oxazine 4/reduced charge montmorillonite dispersions. Emission spectra excited at 575 (**a**) and 615 nm (**b**). Excitation spectra for the emission at 640 nm (**c**). Reduced charge montmorillonites: N1 (*solid line*), N2 (*dashed line*), N3 (*dotted line*), N4 (*scatter*, *open circle*), and N5 (*scatter*, *solid square*)

N1 and N5 samples, of highest and lowest charge densities, respectively. The emission intensities change only negligibly within these groups. Low emission from Ox4/N1 (solid line) can be assigned to the formation of molecular aggregates in this reaction system. The presence of *H*-aggregates in N1 dispersion has been proven by means of the absorption spectroscopy (Figs. 3 and 4). In general, the *H*-aggregates act as efficient fluorescence quenchers [10]. Besides quenching, the formation of the aggregates brings about lower amount of fluorescently active species, which are hypothesized to be mainly isolated (nonaggregated) Ox4 cations and potentially *J*-aggregates. Significant lowering of the *H*-aggregates in RCMs of medium charge reduces fluorescence quenching and increases amounts of the fluorescently active species. The highest fluorescence is observed for the dispersion with N3. Ox4/N4 dispersion exhibits emission intensity similar to Ox4/N2, but the band shifts slightly to lower wavelengths. The position of the band is similar to that observed for the dispersions of low-charge saponite [19]. Further reduction of the layer charge (N5) led to the decrease of the emission approaching levels of Ox4/N1 dispersion. Significantly

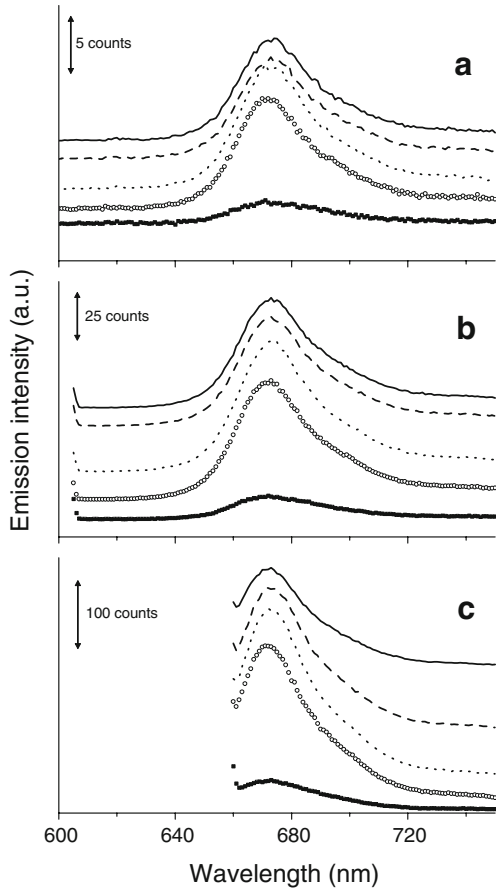

Fig. 9 Fluorescence spectra of oxazine 1/reduced charge montmorillonite dispersions. Emission spectra excited at 560 (**a**), 600 (**b**), and 655 nm (**c**). Reduced charge montmorillonites: N1 (*solid line*), N2 (*dashed line*), N3 (*dotted line*), N4 (*scatter*, *open circle*), N5 (*scatter*, *solid square*)

lower fluorescence in the system with N5 can be assigned to specific colloid properties of this clay mineral specimen. Partial microflocculation of clay mineral particles upon adsorption of the dye cations occur in a N5 aqueous colloidal dispersion. The flocculation can be monitored by means of light scattering, or, if it is more remarkable, visually as sedimentation of clay colloid particles with time. Increasing association between clay mineral particles for the RCM with the lowest layer charge is due to low electrostatic repulsion forces between electric double layers of interacting particles. The repulsive forces can be further weakened upon the adsorption of the organic dyes cations neutralizing diffuse electric double layer. The clay layer association leads to the formation of larger colloid particles with trapped dye cations. This process significantly reduces the fluorescence, which can be explained in terms of two coexistent mechanisms:

1. Fluorescence self-quenching is enhanced due to increasing dye concentration in flocs of clay particles
2. Indirect effect based on light scattering has to be considered as well. Flocs contribute to a lower transparency of RCM colloids due to a stronger light scattering. Trapped dye cations in clay mineral flocs are partially shielded from light used for the excitation. Part of emitted light can be backscattered by colloid particles

Both of the mentioned effects may significantly contribute to the reduction of measured emitted light from Ox4/N5 dispersion. Similar effects have been observed for similar systems with rhodamine dyes [21, 22].

Intensity of emitted light is significantly related to the energy of light used for the excitation. The excitation at 575 nm causes the emission of several times lower intensities than that at 615 nm (Fig. 6). The former excitation wavelength is associated with light absorption of Ox4 dimers, partially overlapped with the absorption high-energy tail of isolated dye cations. Although Ox4 in the N1 dispersion absorbs significantly at 575 nm compared to other dispersions, there is no enhancement of the emission due to excitation at this wavelength. Therefore, the emission as observed in the dispersions with Ox4 is mainly due to electronic transitions in Ox4 monomers. Interestingly, the emission from Ox4 cations is directly related to the amount of monomers (with exception of Ox4/N5). It indicates a negligible role of *H*-aggregates in fluorescence quenching. The *H*-aggregates may be segregated on the surfaces with locally higher charge densities, apart from the monomers, which are present on the surfaces with lower charge densities. Another explanation would be based on the hypothesis that the molecular assemblies formed are not very efficient quenchers. There could be various possibilities to explain this fact. One of the explanations is relationship between the yields of energy transfer processes and spatial orientation of electron transition vectors between interacting molecules. Hence, under certain intermolecular orientation, the energy transfer may lead to relatively low yields. In order to answer, if the orientation of the molecules causes low energy transfer in the case of oxazines, one would have to determine molecular orientation of the cations forming both the *H*-aggregates and monomers. A perpendicular orientation of the Ox4 cations forming *H*-type assemblies was observed for solid films [20]. The dye cations in other forms were almost parallel to clay mineral surface. If identical orientations occur also in colloids would need further study. Problem of determination of molecular orientation in colloids would be in implementing a reliable method to preferably orient clay mineral particles in colloids to measure spectral dichroism.

In order to confirm the origin of the emission at 640 nm, excitation spectra were measured as well (Fig. 8c). Light

emission achieved maximum at the excitation at about 625 nm, which is assigned to dye monomers, as can be verified using absorption spectra measurements (Figs. 3 and 4). Excitation and emission spectra are of the same shape.

Fluorescence spectra of Ox1 in RCM dispersions (Fig. 9) are relatively similar to those of Ox4 (Fig. 6), although the trends in dependence on the layer charge of RCMs are partially different. The difference is mainly due to lower amount of *H*-aggregates formed in Ox1/N1 dispersion. Very low emission was observed for the Ox1/N5 dispersion, which can be explained in terms of poor stability of a N5 colloid, in the same way, as has been discussed for the Ox4/N5 (see above). For other systems (N1–N4), the emission increases with increasing excitation wavelength from 560 to 655 nm (Fig. 9). This is in accordance to the increase of absorbance values at these wavelengths as observed in absorption spectra (Fig. 3). Interestingly, excitations at low wavelengths (560 and 600 nm) led to emission spectra of similar shapes regardless RCM present in the dispersions (with exception of N5). On the other hand, intensity of emitted light was more susceptible to clay mineral template upon the excitation at 655 nm (Fig. 9). Significantly lower emission from Ox1/N1 dispersion was observed, which can be interpreted in terms of partial aggregation of Ox1 and less monomers in N1 dispersions, as has been confirmed using absorption spectroscopy. Relatively high emission from Ox1/N1 dispersion at low wavelengths (560 and 600 nm) indicates low extents or even absence of emission quenching by *H*-type molecular assemblies. The only explanation of relatively high emissions of the Ox1/N1 system excited at 560 and 600 nm is an existence of other luminescent species absorbing light at low wavelengths. These could be *H*-/*J*-type dimers of emission characteristics similar to dye monomers. Potentially, other phenomena such as energy transfer from or to molecular assemblies may occur, which may further complicate the interpretation of fluorescence spectra.

Comparisons of optical properties of oxazine dyes

Cationic oxazines dyes tend to form molecular assemblies in the dispersions of layered silicates. Similar to other types of cationic dyes, the type and amounts of the dye molecular assemblies depend much on the layer charge of inorganic template. *H*-aggregates were primarily formed in the dispersion of layered silicate of the highest charge density. The amount of the *H*-aggregates decreased with decreasing layer charge in favor of isolated dye cations or other molecular assemblies such as *J*-aggregates or *H*-dimers. Ox4 forms much more molecular aggregates than Ox1. This difference can be assigned to the presence of relatively larger hydrophobic groups in Ox1 cation. Lipophilic character of ethyl group probably affects the molecular association in a significant extent. Ethyl groups form van der Waals association with heteroaromatic skeleton in order to reduce unfavorable interactions with water molecules. Consequently, sandwiched-type aggregates are prevented to be formed in Ox1 systems. Inclusion of aliphatic ethyl chains in the intermolecular association may increase the intermolecular distance. It would be larger than if interacting molecules are perfectly flat and heteroaromatic skeletons form perfect sandwich-type arrangements. Larger distance between transition moments would contribute to lower changes of both the absorption and fluorescence spectra. Similar effects have been observed for other types of dyes. Significantly lower aggregation is observed by means of absorption spectroscopy for rhodamine 3B with the presence of four ethyl groups attached to ammonium groups [23]. Rhodamine 3B structure is somehow similar to that of oxazine 1. Presence of bulky groups led to the enhancement of fluorescence of squaraine dyes [24]. More detail studies with other types of dyes have been published elsewhere (e.g., [25, 26]).

Changes in absorption spectra with time prove thermodynamic instabilities of freshly prepared dye/layered silicate dispersions and relatively slow structural rearrangement of the molecular assemblies. This is similar to the systems with other organic dyes. The changes are quite complex and specific to the properties of a layered silicate template.

Fluorescence spectroscopy revealed mostly a slight effect of the properties inorganic component on dyes luminescent properties. The systems with the silicates of medium layer charge exhibit the highest luminescence. In the case of Ox4, a significant quenching is observed due to dye molecular aggregation, whereby the fluorescence of Ox1 is less susceptible to this phenomenon. Dispersions with clay mineral of the lowest charge exhibit low fluorescence yields, which is related to the colloidal properties of the systems.

Overall, the fluorescence of oxazine dyes is relatively high even for the cases, in which the occurrence of the *H*-aggregates was proven. This is in contrast to rhodamine dyes [21, 22] with low emissions occurring for clay mineral dispersions due to formation of dye molecular assemblies and strong fluorescence quenching. This fact makes oxazines dyes potentially suitable candidates for efficient fluorophores in hybrid materials, which are based on layered inorganics and embedded organic dyes. Optical anisotropy and energy transfer processes has been studied for the hybrid films based on clay mineral with embedded Ox4 cations [19, 27]. Ox1 has not been studied so extensively. For the first time, its interesting properties dealing to low molecular aggregation are proven in this paper. Understanding basic principles of the formation of molecular assemblies of fluorescent dyes in clay mineral colloids may help to use these complex systems for the preparation and to control the synthesis of novel hybrid

materials such as clay minerals/organic dyes Langmuir–Blodgett films [28, 29], fuzzy assemblies [30], nanocomposites [31], etc.

Acknowledgement This work was supported by the Slovak Research and Development Agency under the contract no. APVV-51-027405. Support from grand agency VEGA is also acknowledged (project 2/6180/27).

References

1. Dékány I, Szanto F, Weiss A, Lagaly G (1985) Ber Bunsenges Phys Chem 89:62
2. Ras RHA, Németh J, Johnston CT, Dékány I, Schoonheydt RA (2004) Thin Solid Films 466:291
3. Lagaly G, Dékány I (2005) Adv Colloid Interface Sci 114:189
4. Sylven B (1954) Quart J Micr Sci 95:327
5. Hartveit F (1981) J Pathol 134:7
6. Zanini GP, Avena MJ, Fiol S, Arce F (2006) Chemosphere 63:430
7. Kapuscinski J (1990) J Histochem Cytochem 38:1323
8. Hattori S, Sakai K, Watanabe K, Fujii T (1996) J Biochem 119:400
9. Gummow BD, Roberts GAF (1985) Makromol Chem 186:1239
10. Kobayashi T (1996) J-aggregates. World Scientific, Singapore
11. Bergman K, O'Konski CT (1963) J Phys Chem 67:2169
12. Bujdák J (2006) Appl Clay Sci 34:58
13. Bujdák J, Komadel P (1997) J Phys Chem B 101:9065
14. López Arbeloa F, Tapia Estévez MJ, López Arbeloa T, López Arbeloa I (1995) Langmuir 11:3211
15. Bujdák J, Janek M, Madejová J, Komadel P (1998) J Chem Soc Faraday Trans 94:3487
16. Komadel P, Madejová J, Bujdák J (2005) Clays Clay Miner 53:313
17. Gummow BD, Roberts GAF (1986) Makromol Chem 187:995
18. Gomez-Hens A, Aguilar-Caballos MP (2004) Trends Anal Chem 23:127
19. Czímerová A, Bujdák J, Iyi N (2007) J Photochem Photobiol A 187:160
20. Bujdák J, Iyi N (2006) Chem Mater 18:2618
21. Bujdák J, Iyi N, Sasai R (2004) J Phys Chem B 108:4470
22. Bujdák J, Martínez Martínez V, López Arbeloa F, Iyi N (2007) Langmuir 23:1851
23. Bujdák J, Iyi N (2006) J Phys Chem 110:2180
24. Otsuka A, Funabiki K, Sugiyama N, Yoshida T (2006) Chem Lett 35:666
25. Langhals H, Ismael R, Yuruk O (2000) Tetrahedron 56:5435
26. Hachisako H, Yamazaki T, Ihara H, Hirayama C, Yamada K (1994) J Chem Soc Perkin Trans 2:1681
27. Czímerová A, Iyi N, Bujdák J (2007) J Colloid Interface Sci 306:316
28. Ras RHA, Németh J, Johnston CT, Dékány I, Schoonheydt RA (2004) Phys Chem Chem Phys 6:5347
29. Ras RHA, Németh J, Johnston CT, DiMasi E, Dékány I, Schoonheydt RA (2204) Phys Chem Chem Phys 6:4174
30. van Duffel B, Verbiest T, Van Elshocht S, Persoons A, De Schryver FC, Schoonheydt RA (2001) Langmuir 17:1243
31. Schoonheydt RA (2002) Clays Clay Miner 50:411